STM JOURNALS

Journal of
Thin Films, Coating Science Technology and Application

ISSN: 2455-3344
Volume 13, Issue 1, 2026
January–April
DOI (Journal): 10.37591/JoTCSTA

https://journals.stmjournals.com/jotcsta

Review JoTCSTA

Characterization of Polyurethane at Multiple Scales for Erosion Mechanisms Under Sand Particle Impact

Nirmal Sigamani[1,*], Zoubeida Ounaies[2], Ramesh Talreja[3]

Abstract

Thin polyurethane layers have been widely used as erosion-resistant coatings on helicopter rotor blades such as UH-60 Black Hawk and Eurocopter SA 315. Published research has mainly focused on empirical studies that relate the mechanical properties such as rebound resilience and hardness of polyurethane to solid particle erosion resistance. However, polyurethane possesses phase mixing at multiple scales, and thus sand particle erosion resistance also depends on the microstructure and the phase mixing. Hence, it is very important to carry out detailed investigations to understand the step-by-step mechanism of erosion and how it relates to the polyurethane micro-, meso-, and macro-structure. This study carries out systematic investigations on multiple scales using Fourier transform infrared spectroscopy (FTIR) in the micro scale, differential scanning calorimetry (DSC) in the meso-scale, and scanning electron microscopy (SEM) in the macro scale to understand the step-by-step mechanism of erosion and how it is affected by the polyurethane microstructure. The comparison of FTIR results on pre-eroded and eroded films reveals the removal of macromolecular bonds corresponding to soft segments in the microscale. The reduction of the crystalline portion of the soft segment observed from DSC results supports the FTIR findings. SEM images of the eroded specimens are used to correlate the sequence of the damage due to erosion. The observations reveal that after initial ductile deformation of the soft segments on the surface, brittle cracks are formed on the hard segments. The increased exposure to sand particles leads to the formation of fragments containing mainly soft segments, with cracks in the hard segments propagating in a brittle manner. As exposure increases, cracks intersect, and material on the surface gets removed. The removed material mainly contains soft segments, as revealed by the FTIR and DSC results.

Keywords: FTIR analysis, microstructure–property relationship, polyurethane erosion, phase mixing, solid particle erosion

***Author for Correspondence**
Nirmal Sigamani
E-mail: Nirshank@gmail.com

[1]Ph.D. Students, Department of Mechanical Engineering, Pennsylvania State University, State College, PA, 16801, USA.
[2]Professor (Mechanical Engineering) and Associate Director of Materials Research Institute, Pennsylvania State University, State College, PA, 16801, USA.
[3]Professor, Aerospace Engineering and Material Science and Engineering Department, Texas A&M University, College Station, TX, 77843, USA.

Received Date: November 26, 2025
Accepted Date: December 17, 2025
Published Date: January 25, 2026

Citation: Nirmal Sigamani, Zoubeida Ounaies, Ramesh Talreja. Characterization of Polyurethane at Multiple Scales for Erosion Mechanisms Under Sand Particle Impact. Journal of Thin Films, Coating Science Technology and Application. 2026; 13(1): 1–13p.

INTRODUCTION

Sand particle erosion is a severe problem with helicopter rotor blades. There are several methods to evaluate the erosion resistance of the material; the most common method in use consists of sand blasting experiments to simulate erosion conditions [1]. Two major factors affect the erosion process. One factor consists of erosion-causing parameters such as the impacting particle velocity, impingement angle, mass of the silica particles, and their size distribution. Other factors concern material properties such as hardness and rebound resilience. The erosion problem differs from other wear problems in two aspects, namely, the range of the impact angle and the frequency of impact. Abrasion usually happens at very low angles and

low impact velocities [2]. However, erosion is capable of much more damage because of higher impact angles and velocities. Several studies have been carried out for various materials to find the variation of the erosion resistance with the impingement angle. It was found that ductile metals erode significantly at impingement angles in the range 20–30° while brittle metals erode very rapidly near 90°. Also, the sand particle erosion was found to vary drastically with the impact velocity. Furthermore, there exists a threshold velocity for each material above which the erosion rate will increase exponentially. Moreover, the impact velocity of the sand particle and the distribution of the sand particle size in the air media determine the frequency of impact on the coatings [3–6].

Similar studies were conducted for elastomers by Zahavi et al. [7], who detected a variation in the angle at which maximum erosion occurred between hard particles and elastomeric polyurethane coatings. For given erosion parameters, different materials display different levels of erosion resistance, which depends mainly on the material properties, such as hardness and rebound resilience. Hutchings et al. [8] studied the effect of the mechanical properties of polyurethane on its erosion resistance. By keeping the rebound resilience essentially constant, they studied the variation in erosion resistance with variations in hardness, tensile strength, and elastic modulus. The study revealed that hard elastomers had very high recovery times and erosion rates. Elastomeric coatings were proven to be independent of the impingement angle beyond 45°, and the gain of mass was reported to be near 90°. This may be due to the silica particles getting embedded into the coating at normal angles of impact. Hutchings et al. [8] conducted erosion experiments with elastomers having different rebound resilience to study the effect on erosion resistance and found that highly resilient elastomers are very effective for erosion resistance. They also found that the erosion rate varied exponentially with rebound resilience.

Elastomers are generally co-block polymers with two major segments, one of which has a very low glass transition temperature (Tg) (well below room temperature), whereas the other has a Tg well above room temperature. Hence, one phase or segment is highly flexible, whereas the other segment has a rigid crystalline nature. Due to these unique characteristics, elastomers have a greater impact-absorbing capability without losing the modulus of the material; therefore, they are preferred in the aerospace coating industry. Polyurethane (PU) is an elastomer (Figure 1) featuring micro-and nanoscale phase separation between two types of segments. Tocha et al. [9] used transmission electron microscopy (TEM) and atomic force microscopy (AFM) to confirm the structure of PU and found that the soft-to-hard segment phase separation is greatly influenced by the composition and proportion of the hard segment. The possibility of tailoring the morphology of PU combined with its elastomeric behavior makes it a material of choice as a protective coating in several applications, including helicopter blades.

Zahavi et al. [7] explored the mechanism of erosion in polyurethane coatings and found that the propagation of fine cracks from the surface into the bulk led to the formation of fragments. The erosion mechanism is better understood when considering the recovery time. Hard elastomers have higher recovery times and take longer to dissipate the absorbed energy. Hence, when a sand particle impacts a region that has not yet fully recovered, the repeated impact on that region eventually causes plastic deformation, and the material is removed locally. Consequently, solid particle erosion in polyurethane is believed to occur in four stages. Initially, surface cracks are formed by repeated impact, and the cracks tend to propagate by the impact of the sand particles on the existing cracks. Cracks tend to grow on the surface and into the bulk. When the propagating cracks intersect each other, the local material is chipped out of the surface and forms fragments. Finally, under steady-state erosion, the fragments are removed from the surface, causing material loss.

The preceding sections reviewed the three major areas of interest: sand particle erosion parameters, PU morphology, and the current understanding of the mechanism of material removal. The erosion resistance of polyurethane has been approached with a main focus on empirical studies that either assess the effect of crosslinking density and hardness of polyurethane on solid particle erosion resistance or the effect of addition of fillers in improving the erosion resistance [10–11]. In addition, several studies

have been conducted on PU to better understand its morphology and phase separation [12]. Given the unique multiphase structure of PU, it is important to investigate sand particle erosion at multiple scales, rather than just focusing on the loss of material, as has been done so far in the literature. A proper understanding of the microstructural changes due to erosion is crucial for addressing unresolved problems in aerospace design and maintenance.

This study systematically investigates the mechanisms of sand particle erosion in polyurethane (PU) films and the influence of microstructural changes induced at different stages of erosion. The effect of PU morphology was assessed by considering PU films of different hardness (and hence different % HS) and by investigating two different PUs: polyester-based and polyether-based.

The samples subjected to erosion were characterized before and after erosion using different techniques, such as DSC and FTIR. The strategy is to analyze the results from various characterization techniques to develop an understanding of the erosion mechanisms at various scales, from the bond level to the microstructure and macro levels. Recently, Zhang et al. [13] found that the thickness of polyurethane coatings also plays a vital role in the erosion resistance under solid particle impact. In polyurethane, these macroscale properties are generally the result of microscale phase mixing between soft and hard segments. Therefore, Zhang et al. [14] studied the damage to the microstructure of polyurethane using FTIR and XPS to relate the changes in the macromolecular chain to the macroscopic abrasive erosion performance. However, to the best of our knowledge, no study has reported a relationship between the failure mechanism during solid particle erosion and the morphology and microstructure of PU. To fill this gap, we subjected commercial PU thin films to sand blasting experiments and systematically studied the resulting damage, as shown in Figure 1.

EXPERIMENTS

Material

Thin polyurethane films with thicknesses ranging from 0.3–0.5 mm were supplied by Deerfield Urethane Ltd. and 3M Ltd. for this research. The films were pure thermoplastic elastomers with no additives. Four cases, two polyester-based and two polyether-based, were considered in this study. The hardness of the films varied between 80 Shore A and 90 Shore A, ensuring sufficient variation in the microstructure of the films under study. The two polyester-based PU films are named PS-80 and PS-85, indicating the chemical composition (PS for polyester) and the hardness (the numerical value). Similarly, the two polyether-based PUs are named PT-82 and PT-90. The mechanical properties of the films are listed in Table 1.

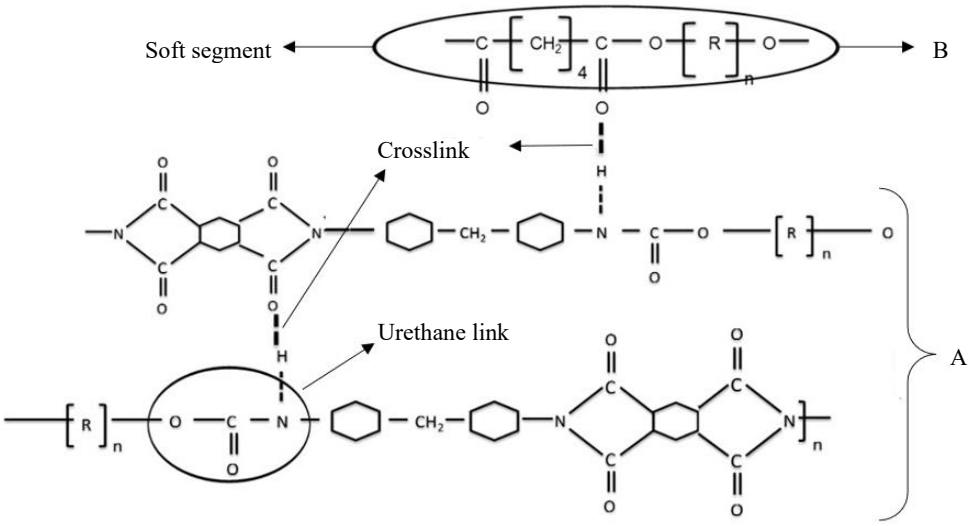

Figure 1. Chemical structure of PU.

Sand Blasting Experiments

The PU thin films were subjected to sand blasting experiments as per ASTM-F1864 under simulated conditions at the University of Dayton Research Institute. The PU films under study were exposed to an impact velocity of 500 mph and an impact angle of 30º. Two different types of sand particles were used: Gulf sand (240–550 μm) and Round Sand (177–250 μm). In addition, the films were subjected to five different mass loadings of sand particles: 0.5, 1, 2, 10, and 20 g/cm².

Techniques for Characterization

An FTIR Spectrometer (Nicolet 380) in ATR mode was used to characterize the pre-erosion and post-erosion film specimens. A DSC (Q-20, TA Instruments) was used to study the thermal properties and analyze the extent of damage on the surface of the PU films under a standard heating rate of 10°C/min. SEM of the surface and the fracture surface was conducted using SEM-JOEL-6400 after the thin films were coated with a thin layer of platinum [15].

RESULTS AND DISCUSSIONS

FTIR Analysis

Figures 2 and 3 show the FTIR results of the pre-erosion film samples near the N–H and C=O bonds, which are used to identify the differences between the types of PU. All the films showed a peak at 3340 cm^{-1} (bonded N–H), confirming that all the N–H bonds in the urethane link were involved in crosslinking. There was a clear difference in the FTIR results near the C=O bond between the polyester-based and polyether-based PU. The two polyester-based films, PS-80 and PS-85, showed higher peaks for free C=O at 1730 cm^{-1} than for bonded C=O at 1700 cm^{-1}. In polyester-based PU, the free C=O bond is found in the ester linkages of the soft segment, whereas the bonded C=O is found in the urethane linkages of the hard segment. However, polyether-based PU does not contain carbonyl linkages (C=O) in the soft segment ether linkages (C–O–C). For polyether-based PU, both N–H and C=O represent hard segments. The soft segment in the polyether-based PU is characterized by the C–O–C bond, which gives a peak at 1230 cm^{-1}. Thus, FTIR can identify the type of PU, and the FTIR results of the pristine film samples were compared with the FTIR results of the eroded film samples to analyze the extent of the damage to the macromolecular bonds.

Table 1. Mechanical properties of the PU films.

Properties	PS-80	PS-85	PT-82	PT-90
Type	Aliphatic Polyester	Aromatic Polyester	Aromatic Polyether	Aromatic Polyether
Hardness (Shore A)	80	85	82	90
Ultimate Tensile Strength (MPa)	35.02	68.94	61.36	66.87

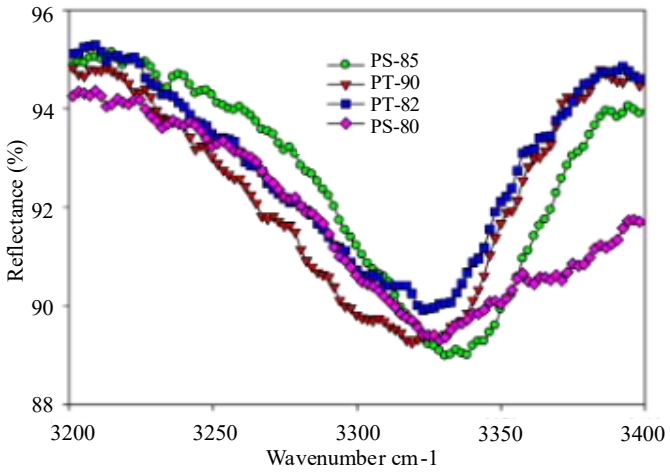

Figure 2. FTIR results of the polyurethane thin films near the N-H region.

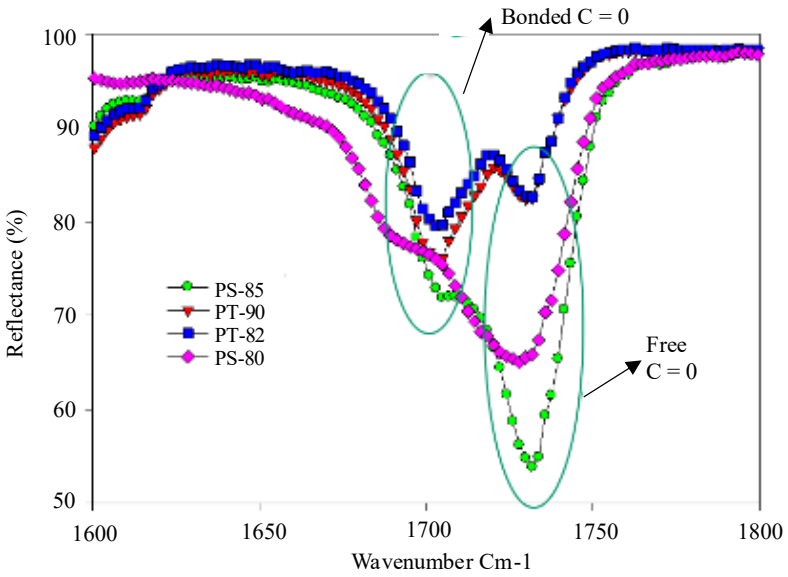

Figure 3. FTIR results of the polyurethane thin films near the C=O region.

The FTIR results of the eroded films of PS-80 and PS-85 subjected to various mass loadings indicate that the free C=O bond at 1730 cm^{-1} gradually reduced with an increase in the mass loading, as shown in Figures 4 and 5. The N–H bond at 3340 cm^{-1}, which is found in the hard segments, did not show any reduction, as shown in Figure 6 for PS-85, suggesting that the removal of the hard segment was minimal. However, the trends differed between the polyester-based and polyether-based PU films. Polyester-based PU films, such as PS-80 and PS-85, which have significantly higher amounts of free C=O, have shown a significant reduction in the free C=O bond. These results suggest that the soft segments containing free C=O bonds in the polyester-based PU were gradually removed from the surface during erosion, and the damage was mainly caused during the early stages of erosion up to 2.0 g/cm^2.

Among the four samples tested in the sandblasting experiment, the PS-80 film demonstrated greater resistance to erosion than the other films, with less mass loss from the material. The FTIR results of PS-80, PS-85, and PT-90 for different wavelength regions correspond to the C=O and N–H bonds. Figure 4 shows the remarkable destruction of the free C=O bonds corresponding to the soft segments due to erosion in the PS-80 samples. Similarly, minimal changes in both the free and bonded C=O corresponding to the hard segments were observed in the hardest film PT-90 (Figure 7).

This behavior suggests a correlation between the observed erosion resistance and the type of microstructure damaged during erosion. As discussed earlier, there exists an incubation period in the erosion process in which the material requires a certain amount of energy to first roughen the surface, and then the steady-state erosion and material removal occur.

The FTIR results showing damage in the soft segment at earlier stages of erosion suggest that the high impact energy imparted on the surface of the films is absorbed by the macromolecular chains corresponding to the soft segment. Additionally, because of the flexible nature of the soft segment, these segments undergo ductile deformation and absorb more energy before they fail.

Damage to the microstructure of polyether-based PU films exhibited different behavior compared to that of polyester-based PU films. The N–H and C=O bonds (both free and bonded) did not show any reduction in the intensity of the peaks corresponding to them. However, the peaks corresponding to CH2 (2860 cm^{-1}) and C–O–C (1250 cm^{-1}) groups were reduced due to erosion. The C–O–C bond represents a soft segment in polyether-based PU films. The increase in the C–O (1100 cm^{-1}) groups seen in Figure 8 suggests that the C–O–C bond has been broken down, leading to the formation of more C–O. Moreover, the C–N bond has also shown a tremendous reduction due to erosion.

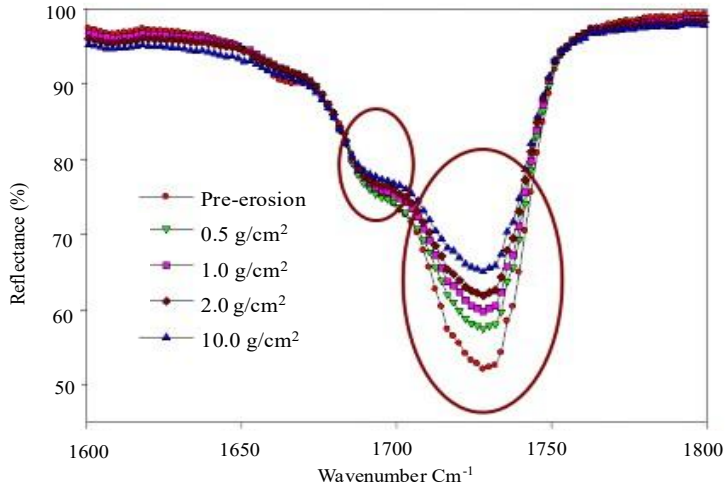

Figure 4. FTIR results near the C=O region for different mass loadings of PS-80.

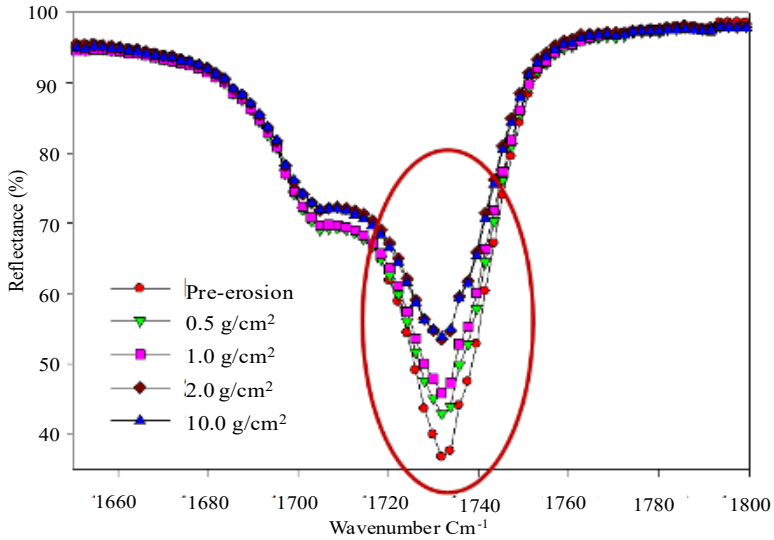

Figure 5. FTIR results near the C=O region for different mass loadings of PS-85.

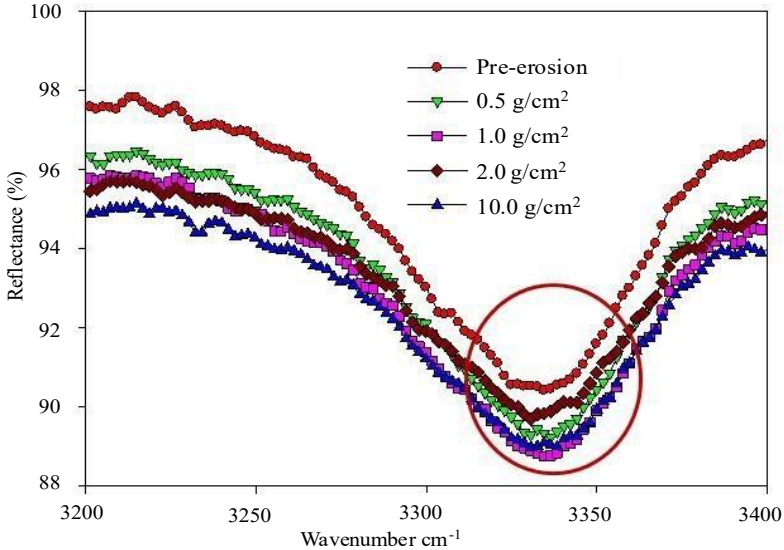

Figure 6. FTIR results near the N–H region for different mass loadings of PS-85.

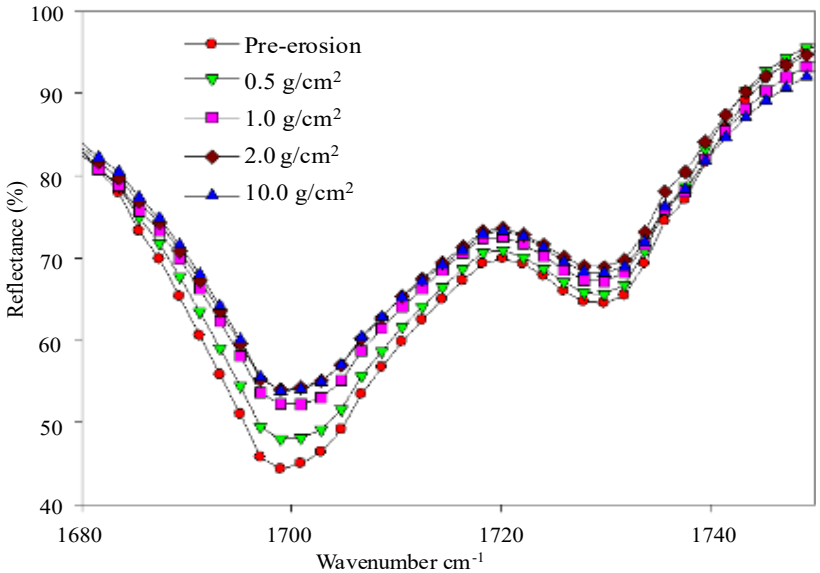

Figure 7. FTIR results near the C=O region for different mass loadings of PT-90.

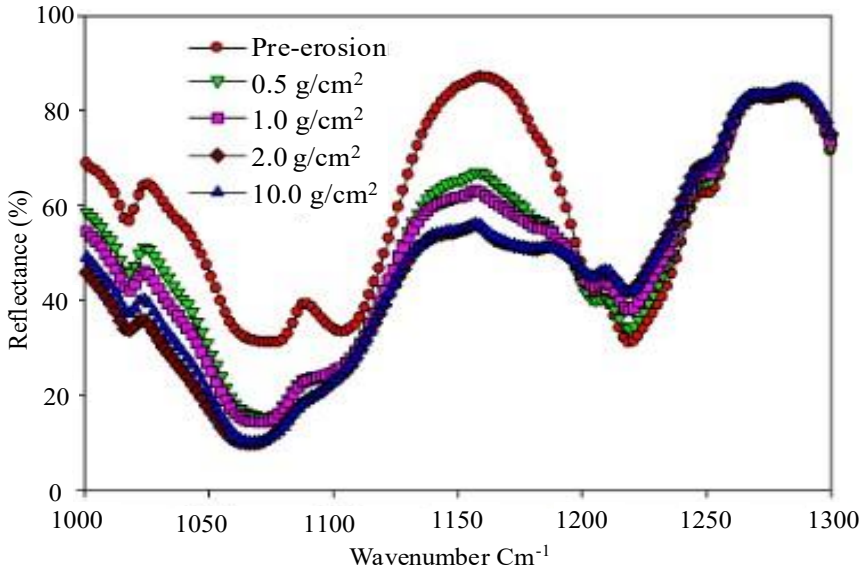

Figure 8. FTIR results near the C–O–C and C–O region for various loadings of PT-90.

Hence, it is likely that the breakage of the bonds occurred gradually in both the soft and hard segments of these polyether-based PU films owing to exposure to sand particle impact. Some part of the hard segment or the cross-link that connects the two phases gets damaged, leading to a heavy amount of material removal when exposed to more than 20 g/cm². There are two possibilities for the location of the damage. The first possibility is the breakage of the covalent bond C–N, as shown in Figure 1, connecting the hard and soft segments. The second possibility is the breakage of C–O–C bonds in the soft segment region, leading to small fragments of soft segments on the surface of the eroded films. The C–N bond has the lowest bonding energy and is therefore the most susceptible to failure owing to impact.

Differential Scanning Calorimetry

The differential scanning calorimetry (DSC) results of pristine film PT-90 when heated up to 375°C and cooled back to –90°C in a nitrogen atmosphere revealed that the soft segment did not melt in the first cycle because their movement was hindered by the cross-links between the hard segments. These

cross-links decompose at 350°C in the first cycle, allowing the soft segments to crystallize at approximately 10°C upon cooling and then melt at approximately 20°C in the second heating cycle, as shown in Figure 9. The DSC results of PT-90, which was subjected to 20 g/cm² erosion, showed a reduction in the soft segment melting peak in the second cycle compared with 0.5 g/cm² exposure, as shown in Figure 10. The reduction in the intensity of the peak indicates a reduction in the crystalline portion of the soft segment after erosion. This supports the FTIR finding that the soft segments were preferentially removed compared to the hard segments.

Scanning electron microscope (SEM) was used to observe the damage caused by erosion on the surface of the eroded films. All the films showed a considerable amount of ductile deformation during the initial stages of erosion. The formation of brittle cracks was distinct for the polyester- and polyether-based films. The film with a very high hardness exhibited a high density of brittle cracks. The films subjected to exposure of more than 10 g/cm² showed that further ductile deformation had taken place even after brittle cracking on the surfaces. The films with maximum silica exposure show the intersection of the brittle cracks and the opening of the cracks.

Scanning Electron Microscope

SEM images were used to observe the sequence of damage in both polyester- and polyether-based PU, as well as the variation in surface damage between the softer and harder films. Figure 11 shows the sequence of damage due to erosion by Gulf sand in the PS-80 films, which demonstrated the best resistance to erosion. The initial stages showed more ductile deformation on the surface.

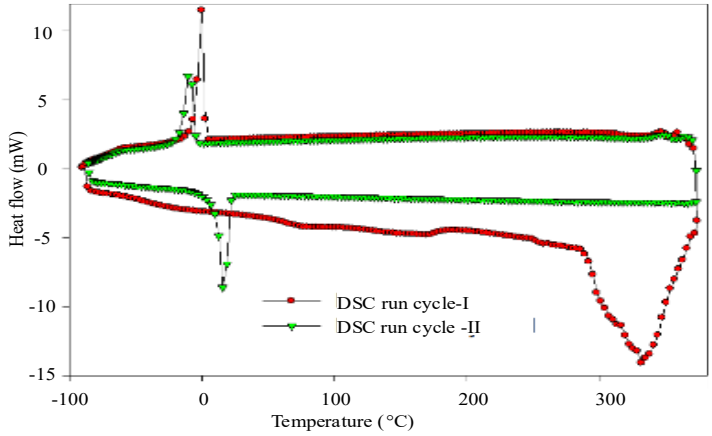

Figure 9. Two DSC cycles showing the melting peak in the 2nd cycle.

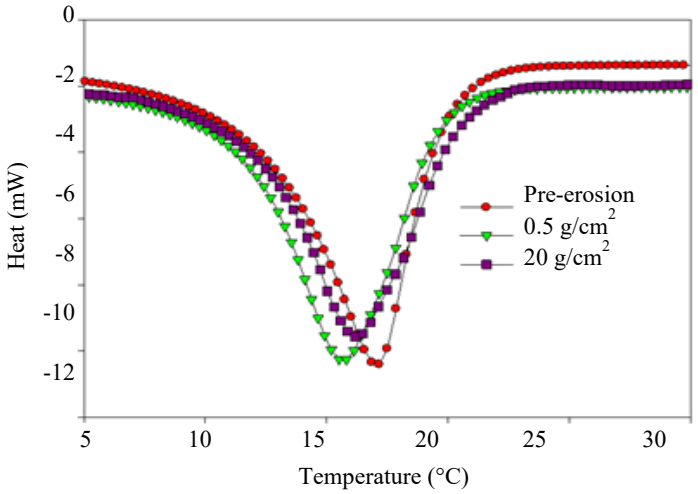

Figure 10. Comparison of the melting peak of soft segments for different mass loadings on PT-90.

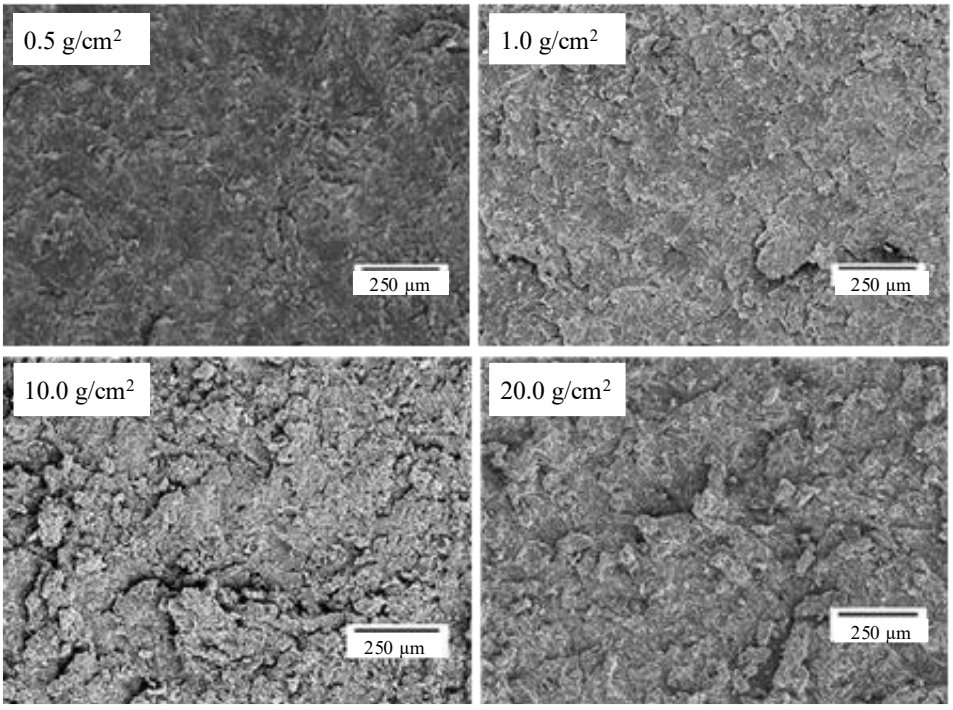

Figure 11. SEM images showing the stages of erosion on the PS-80 film surface.

The formation of fragments is observed at later stages, and at these stages, there are fewer brittle cracks on the surface. The sequence of damage due to erosion by Gulf sand in polyether-based PT-90 is shown in Figure 12. Very little ductile deformation was observed during the initial stages, in which bond breakage was observed by FTIR on PT-90. A large number of relatively large brittle cracks were observed in the subsequent stages. This particular film showed severe damage with evidence of huge cracks on the surface due to erosion at 20 g/cm². The final stage shows the portion of the material loosely adhered to the surface and ready to be removed owing to the intersection of cracks.

In general, polyester-based PU films show a considerable amount of ductile deformation during the initial stages of erosion, which correlates with the ductile deformation in the soft segment identified by FTIR. The formation of fragments, which mainly contain soft segments, is the primary mechanism of material removal in these films. In contrast, polyether-based PU films did not show much ductile deformation on the surface; instead, brittle cracks were found during the initial stages of erosion. The intersection of brittle cracks is the main mechanism for the removal of these films. Materials with high hardness exhibited a high density of brittle cracks. Thus, the variation in the composition and microstructure changed the erosion mechanism, as observed in these films. Polyester-based PU films with low hardness exhibited good resistance to erosion, whereas polyether-based PU with the highest hardness underwent severe damage.

The SEM images at higher magnification revealed a change in the erosion mechanism of the polyester-based and polyether-based PU films. Figure 13 shows the fragments attached to the surface of the PS film and the formation of brittle cracks in the PT film at the initial stages of erosion at 1.0 g/cm² exposure of gulf sand. Similarly, at higher exposures, Figure 14 shows the deformation of the material at the surface, whereas the intersection of brittle cracks is visible for the PT film.

The SEM was extended to observe the extent of the damage in the bulk. The eroded films were fractured under liquid nitrogen (LN2), and the cross-section was observed using SEM. The observations revealed that the damage on the surface travelled into the bulk. Cracks were formed owing to the erosion travelling into the bulk, and some other brittle cracks were found in the cross-section, as shown in Figure 15.

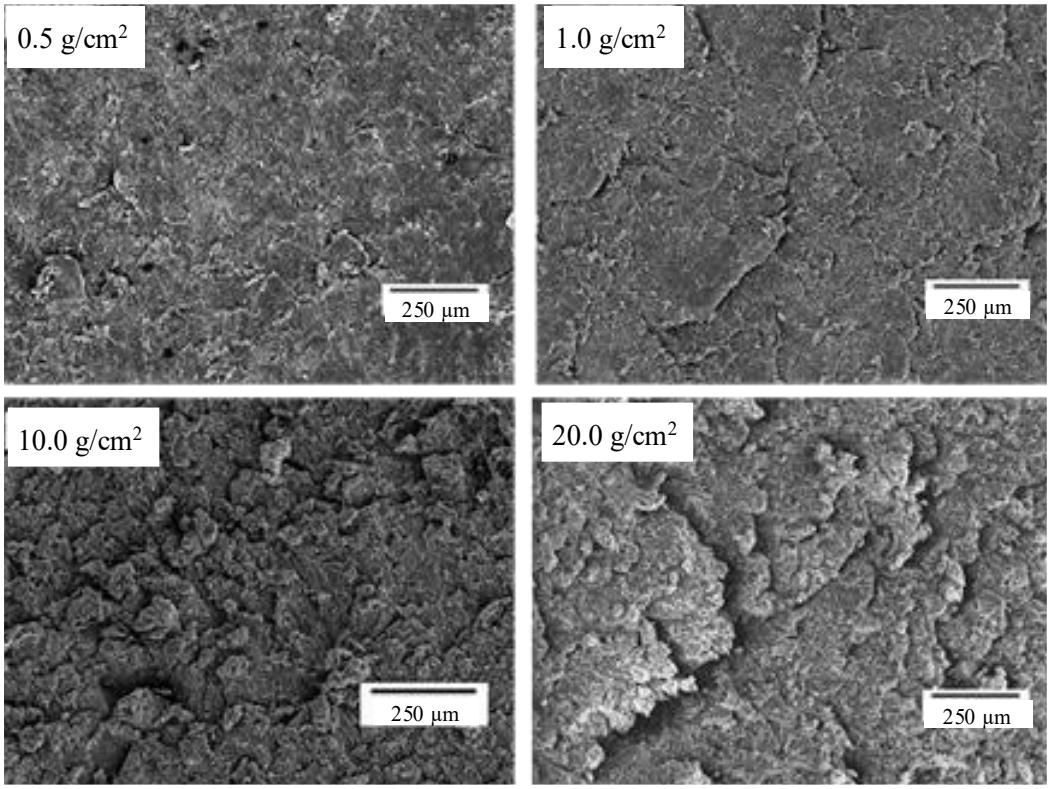

Figure 12. SEM images showing the stages of erosion on the PT-90 film surface.

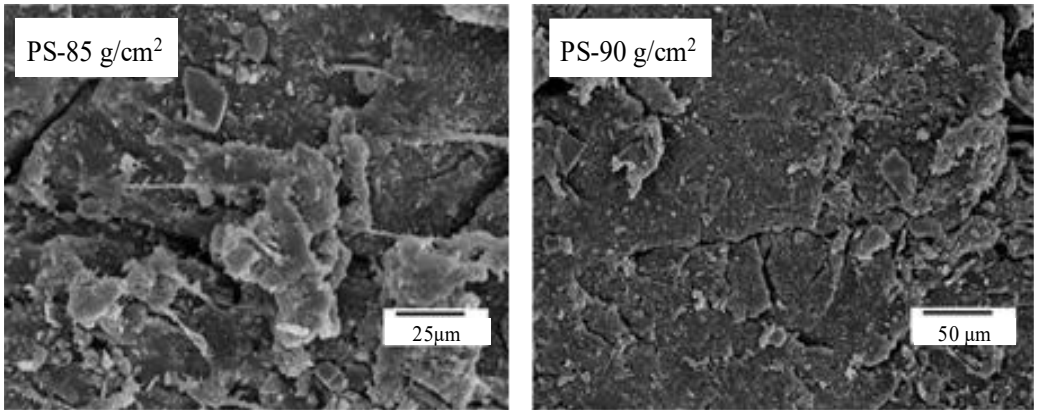

Figure 13. Comparison of initial damage in PS and PT films at earlier stages.

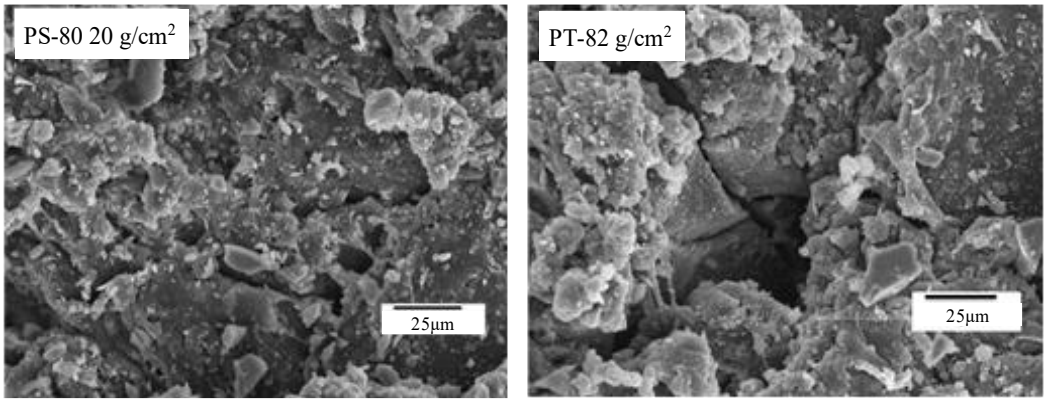

Figure 14. Comparison of damage at higher exposures in PS and PT films.

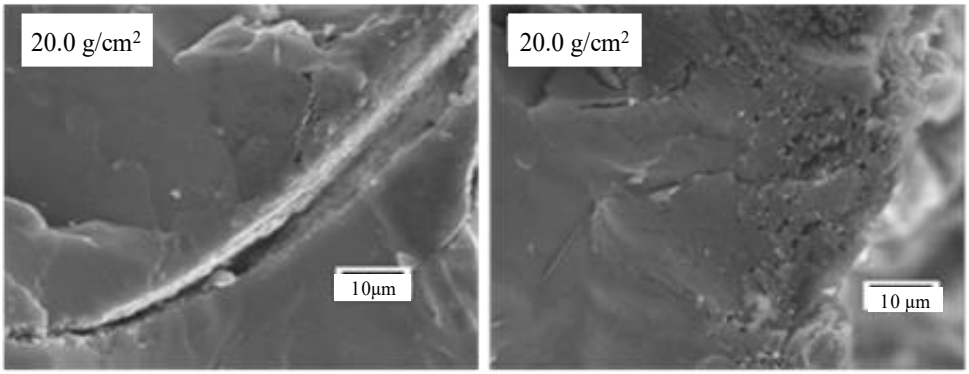

Figure 15. SEM images of the cross-section of the PT-90 film exposed to 20 g/cm^2.

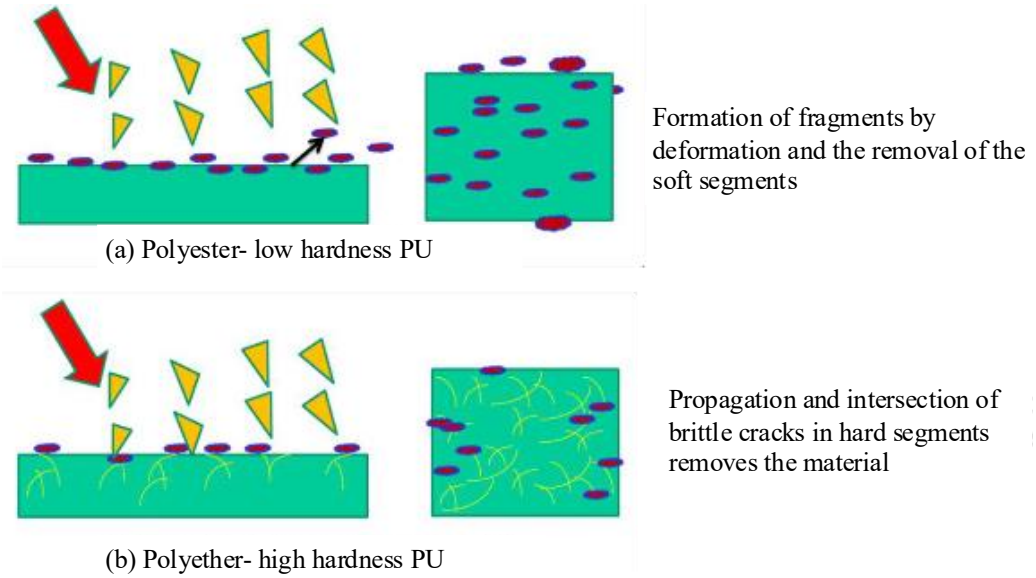

Figure 16. Mechanism of material removal of two types of PU films.

There is a possibility that a few cracks might have formed while the films were fractured under LN2; however, the cracks formed due to sand particle erosion were distinct from the brittle cracks formed while fracturing. The brittle cracks formed due to fracturing were so sharp that little or no gap was observed between the crack surface and did not originate from the surface. The pre-existing cracks due to erosion always travel from the surface into the bulk in a brittle manner with no plastic deformation near the crack tip. In addition to the large cracks in the bulk, the intersection of minute cracks beneath the surface is also visible in Figure 15. These two observations represent the two main mechanisms of material removal: the intersection of brittle cracks in the bulk and the formation of fragments by minute cracks beneath the surface. The mechanism of material removal owing to sand particle erosion for polyester-based PU and polyether-based PU is illustrated in the illustration (Figure 16).

The effect of damage by round sand was also observed to compare the effect of particle shape on the erosion of the films. Figure 17(a)–(d) shows the surface of all four films exposed to a maximum loading of 20 g/cm² by the round sand. The images reveal that the damage is minimal relative to exposure to Gulf sand. The round sand media after 20 g/cm² exposure only roughened the surface, and no severe damage was observed that could lead to material removal from the surface. There were no brittle cracks on the surface, even for the hardest material. This result suggests that the brittle cracks on the films exposed to Gulf sand might have originated from the angular sand particles impinging on the hard segments on the surface.

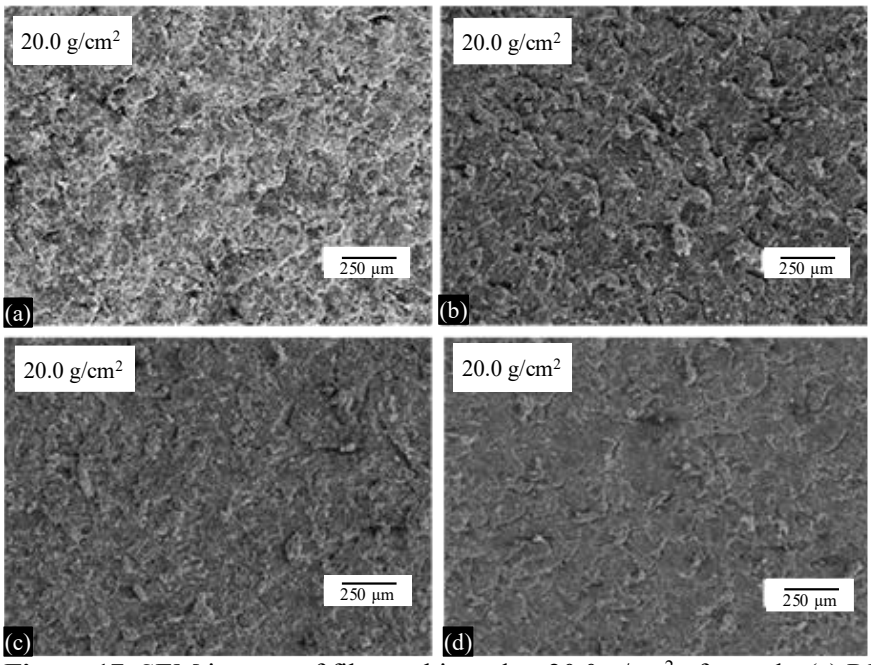

Figure 17. SEM images of films subjected to 20.0 g/cm^2 of rounds. (a) PS-80; (b) PS-85; (c) PT-82; and (d) PT-90.

CONCLUSION

Detailed investigations were performed on both pristine and eroded PU films to detect microstructural damage due to erosion. FTIR spectroscopy was used to document the signatures of the pristine films. Sand particle erosion tests were conducted at 500 MPH, at an impact angle of 30°, with two different sand media: round sand and golf sand. The test specimens were exposed to each sand medium at different mass loadings ranging from 0.5 to 20 g/cm².

The tools of characterization used on the pristine polyurethane were once again used on the eroded specimens to compare the pre- and post-erosion findings. The FTIR results for the eroded films revealed the removal of macromolecular bonds corresponding to the soft segments. In polyester-based PU, the peaks corresponding to free C=O and bonded C=O in the soft segments decreased, whereas the N–H peak showed an insignificant reduction. In general, polyester-based PU showed better resistance to erosion than polyether-based PU. This destruction of the C=O bonds suggests that damage in the soft segment leads to an overall better erosion resistance, as the soft segments are flexible and absorb more impact energy before failure. In polyether-based PU, the breakage of bonds such as C–O–C and C–N, corresponding to both soft and hard segments, is observed. The removal of these bonds from the surface of polyether-based PU owing to erosion is marginal compared to the removal of free C=O bonds in polyester-based PU. The reduction in the crystalline portion of the soft segment observed in the DSC results supports the FTIR findings.

SEM images of the eroded specimens were used to correlate the sequence of damage owing to erosion to the PU microstructure. The observations revealed that after the initial ductile deformation of the soft segments on the surface, brittle cracks were formed in the hard segments. The increased exposure to sand particles leads to the formation of fragments containing mainly soft segments, whereas the cracks in the hard segments tend to propagate in a brittle manner. When the intersection of the cracks occurs at longer exposures, the material on the surface is removed, and it mainly contains soft segments, as revealed by the FTIR and DSC results.

Thus, using the above techniques, the breakage of the macromolecular bond, ductile deformation, and cracks on the microscale were observed. The mechanism of material removal has been mostly

deduced using FTIR. The damage due to erosion starts with bond breakage, leading to various mechanisms, such as the formation of fragments and intersection of brittle cracks, which cause material removal from the surface.

Acknowledgement

The authors acknowledge the financial support provided by the Texas Center for Applied Technologies (TCAT). The authors thank 3M Company and Deerfield Urethane Ltd. for supplying polyurethane films for this study and Dr. Andy Phelps (UDRI) for carrying out sandblasting experiments on the PU films.

REFERENCES

1. Li J, Hutchings IM. Resistance of cast polyurethane elastomers to solid particle erosion. Wear. 1990;135:293-303. doi:10.1016/0043-1648(90)90032-6.
2. Arnold JC, Hutchings IM. The mechanisms of erosion of unfilled elastomers by solid particle impact. Wear. 1990;138:33-46. doi:10.1016/0043-1648(90)90166-8.
3. Born L, Hespe H, Crone J, Wolf KH. The physical crosslinking of polyurethane elastomers studied by X-ray investigation of model urethanes. Colloid Polym Sci. 1982;260:819-828. doi:10.1007/BF01419091.
4. Preece CM, Macmillan NH. Erosion. Annu Rev Mater Sci. 1977;7:95-121. doi:10.1146/annurev.ms.07.080177.000523.
5. Spathis G, Niaounakis M, Kontou E, Apekis L, Pissis P, Christodoulides C. Morphological changes in segmented polyurethane elastomers by varying the NCO/OH ratio. J Appl Polym Sci. 1994;54:831-842. doi:10.1002/app.1994.070540701.
6. Lee DK, Tsai HB. Properties of segmented polyurethanes derived from different diisocyanates. J Appl Polym Sci. 2000;75:167-174. doi:10.1002/(SICI)1097-4628(20000103)75:1<167::AID-APP19>3.0.CO;2-N.
7. Zahavi J, Schmitt GF. Solid particle erosion of reinforced composite materials. Wear. 1981;71:179-190. doi:10.1016/0043-1648(81)90337-9.
8. Hutchings IM, Deuchar DWT, Muhr AH. Erosion of unfilled elastomers by solid particle impact. J Mater Sci. 1987;22:4071-4076. doi:10.1007/BF01133360.
9. Tocha E, Janik H, Debowski M, Vancso GJ. Morphology of polyurethanes revisited by complementary AFM and TEM. J Macromol Sci B. 2002;41:1291-1304. doi:10.1081/MB-120013098.
10. Arjula S, Harsha AP, Ghosh MK. Solid-particle erosion behavior of high-performance thermoplastic polymers. J Mater Sci. 2008;43:1757-1768. doi:10.1007/s10853-007-2405-0.
11. Vu-Khanh T, De Charentenay FX. Mechanics and mechanisms of impact fracture in semi-ductile polymers. Polym Eng Sci. 1985;25:841-850. doi:10.1002/pen.760251309.
12. Woo EJ, Farber G, Farris RJ, Lillya CP, Chien JCW. Structure-property relationships in thermoplastic elastomers: I. Segmented polyether-polyurethanes. Polym Eng Sci. 1985;25:834-840. doi:10.1002/pen.760251308.
13. Zhang N, Yang F, Li L, Shen C, Castro J, Lee LJ. Thickness effect on particle erosion resistance of thermoplastic polyurethane coating on steel substrate. Wear. 2013;303:49-55. doi:10.1016/j.wear.2013.02.022.
14. Zhang SW, He R, Wang D, Fan Q. Abrasive erosion of polyurethane. J Mater Sci. 2001;36:5037-5043. doi:10.1023/A:1011814506377.
15. Coad EJ, Pickles CSJ, Seward CR, Jilbert GH, Field JE. The erosion resistance of infrared transparent materials. Proc R Soc Lond A Math Phys Eng Sci. 1998;454(1968):213-238. doi:10.1098/rspa.1998.0155.

